Stimulated Enhancement of the Lipid Accumulation of Yeast, *Lipomyces starkeyi* in Dielectric Barrier Discharge at Gas/Liquid Boundary

Yurika KOMORI, Hiroshi OKAWA and Tetsuya AKITSU[1)]

Happy Science University, 4427-1 Hitotsu-Matsu Hei, Chosei-Gun, Chiba 299-4325, Japan
[1)]*University of Yamanashi, Professor EMERITUS, 4-3-11 Takeda, Kofu, Yamanashi 400-8511, Japan*

(Received 17 June 2022 / Accepted 26 September 2022)

In this study, we investigated the enhancement of cellular lipid that forms in *Lipomyces starkeyi* under the electro chemical stimulation by discharge in the dielectric barrier electrode at a gas-liquid boundary. The plasma injection sequence and composition of recovery media were optimized for the minimum deterioration of cellular density and maximum increase in the lipid volumes. Under optimum conditions, the volume of lipid globules increased to 1.35 and the count of cells per milliliter to 1.16.

Keywords: atmospheric-pressure plasma, air/water interface, *Lipomyces starkeyi*, plasma-stimulation

DOI: 10.1585/pfr.17.1406109

1. Introduction

Lipomyces starkeyi is a lipid accumulating yeast isolated from soil, and it has attracted attention as a replacement product for vegetable oils [1]. The composition of the lipid contains an unsaturated fatty acid, such as palmitic and oleic acid, in a composition similar to palm oil. The search for new species of this yeast and the optimum fermentation conditions has been investigated. The problem in this study can be summarized in the following three points: 1. the selection of yeast with high efficiency, 2. the optimization of the media and the comparison of growth with inorganic substances, and 3. the development of a high-energy-efficiency lipid globule extraction method. Naganuma *et al.* [2–4] and Yanagiba *et al.* [5–7] have investigated the selection of optimum species and culture methods. The accumulation of triacylglycerols (TAGs) is estimated in this study based on the volume of lipid globules observed under microscopy. We conducted experiments to stimulate lipid formation through plasma exposure. For the decomposition of polycyclic aromatic compounds, plasma streamers in water and discharges in bubbles generate oxygen radicals, such as OH^*. OH radical was detected by the photoluminescence in [8] and the radical degradation of organic compounds [9, 10], the antimicrobial activity in plasma-treated water [11]. Locke *et al.* [12,13] presented a reaction scheme in a water streamer. In this study, we present a method for enhancing the production of yeast-bearing lipids using dielectric barrier discharge plasma at a gas–liquid boundary.

2. Material and Method

2.1 Microbial and incubation conditions

The strain used in the following experiment was *Lipomyces starkeyi* CBS 1807Ⓣ, following the optimized conditions of the culture fixed at a temperature (28°C) and stirred in a custom-made shaker. The frequency is described in the caption of the individual case.

2.2 Plasma injection at the air/liquid boundary

Plasma treatment was performed on a 5 mL culture solution for plasma-treated media and yeast suspension in a 30 mL test tube.

Figure 1 shows a schematic of the atmospheric pres-

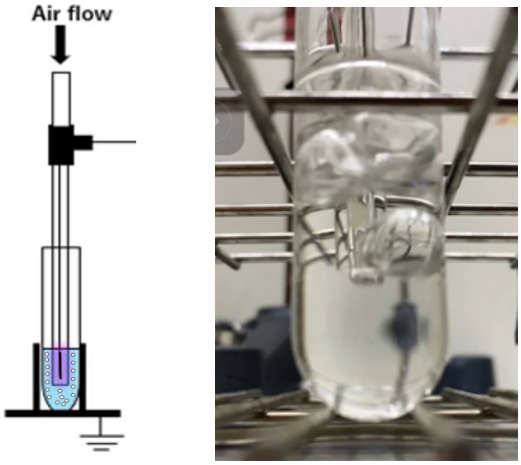

Fig. 1 Plasma treatment in the bubble.

author's e-mail: yurika.0806.canon@icloud.com

Table 1 Operational conditions of the plasma source[a].

Pulse repetition rate	16.88 kHz
Operational time	5 s or otherwise specified
Gas, flow rate[c]	Dry air, 500 (mL/min)

a: Type LHV-10AC-24, b: Type LHV-13AC (Logy Electric Co. Tokyo, Japan).

c: Piezo-electric mass flow controller CMQ (Yamatake).

Table 2-a 1/2YM medium: Standard composition.

Composition	Weight (g/L)
Yeast extract	1.5
Malt extract	1.5
Peptone	2.5
Glucose [a]	4.0
(Agar)[b]	20

a: basic composition; b: the solid medium case.

Table 2-b YPD medium: Special composition.

Composition	Weight (g/L)
Yeast extract	1.5
Peptone	2.5
Glucose [a]	20
(Agar)[b]	20

a: basic composition; b: the solid medium case.

sure air plasma generator. The discharge section consisted of a quartz tube with an outer diameter of 4.0 mm and an inner diameter of 2.0 mm. The high voltage electrode is made of W/5%Re wire with a diameter of 0.6 mm. Dielectric barrier discharge occurs between the inner surface and a high-voltage electrode located in the glass tube. The outside of the glass tube is capacitively coupled to the ground potential. The gas flow produced 4.5 bubbles per second in slow motion. The average diameter of the bubbles was 8.8 mm. The plasma source was driven with a flyback transformer oscillator generating a pseudo-sinusoidal high-voltage pulse. Table 1 shows the operational conditions. The controllability at low power output is what differentiates the two inverters.

2.3 Incubation medium

According to the experiment, 1/2YM and YPD media developed and adjusted in the laboratory were used. The difference in the composition in Tables 2-a and 2-b is the relative amount of glucose, demonstrating the relationship between glucose oxygen and growth obstruction.

2.4 Measurement of the volume of lipid globules and statistical assessment

The volume of the lipid globules was measured using the micrograph method [7]. Figure 2 describes the flow of processing. The preparation of the sampled mixture was

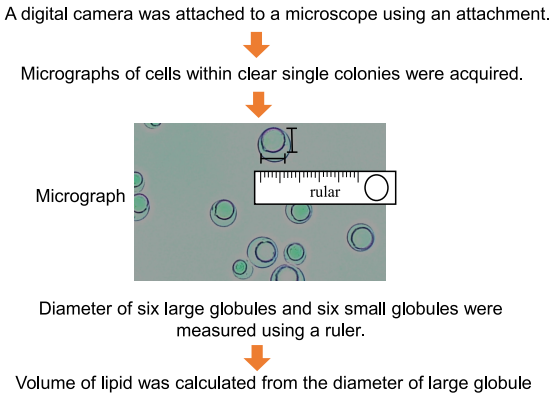

Fig. 2 Measurement of fat the globule volume. A digital camera system Moticam1080 was attached to a microscope AE2000 installed with an objective lens LWDPL, Ph40X (SHIMADZU Co. Kyoto, Japan).

set on a digital image microscope. The samples were cultivated in two groups of three test tubes in parallel. The average and error bars were calculated for large and small cell images. The average and standard errors are displayed in the error bar in the figure. The Dunnett test was performed for the statistical differences among multiple subjects.

The Dunnett test indicated three types of significance levels, which are shown in Figs. 5 and 6 by asterisks: $*p < 0.05$; $**p < 0.01$; $***p < 0.001$.

3. Experimental Results

3.1 Yeast growth curve

Figure 3 (Table 3) shows a typical growth curve of yeast, *Lipomyces starkeyi* in a 1/2YM medium.

The solid line and filled circles represent the number of cell counts (10^8/mL), and the bar graph shows the lipid globule volume. The bar graph represents the volume (μm^3) of the lipid globule. Figure 3 (Table 3) shows the evolution of the volume of the lipid globule and the count of cells after the start of the incubation cycle.

In this case, the logarithmic increase in the cells was observed in the initial 24 h. After 48 h, the increasing rate in the population gradually decreased. The volume of lipid globules must increase continuously after this saturation. The optimization of the incubation condition is to increase the volume of lipid globules.

3.2 Nitrogen radicals in the plasma-treated water

Microbial sterilization using plasma-treated water and the stimulation of enhanced propagation in low-concentration exposure have been reported [9, 10]. Figure 4 (Table 4) shows the concentration of the nitric acid and nitrous acid in the plasma-treated distilled water in the dielectric barrier discharge (DBD mode) and the transfer type arc (ARC mode), respectively. In this experiment, the

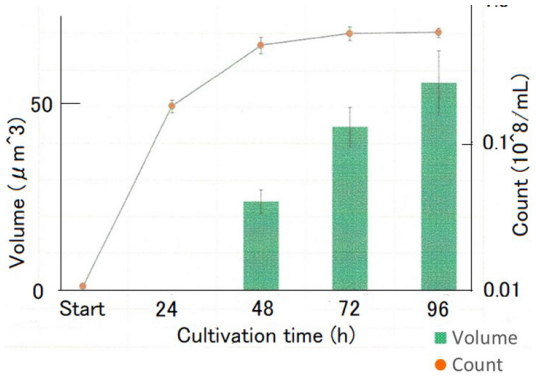

Fig. 3 Typical incubation curve. Bar graph: globules volume (μmm^3). Filled circles: count of cells (10^8/mL).

Table 3 Evolution of the volume of lipid globules.

Cultivation time (h)	24	48	72	96
Volume (μm^3)	–	24.2	44.4	56.6
Count of cells (10^8 cells/mL)	0.18	0.47	0.56	0.57

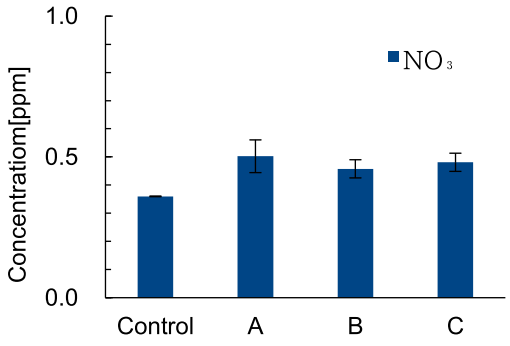

(a)

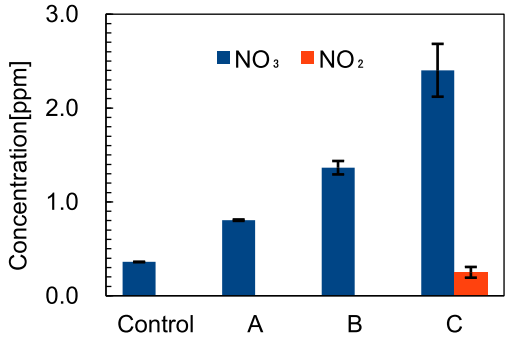

(b)

Fig. 4 Comparison of the concentration of nitric acid and nitrous acid in (a) DBD mode and, in optimized conditions, (b) ARC-mode discharge.

Table 4 Concentration of nitric acid ions.

DBD mode	Control	A	B	C
NO_2	0.36	0.50	0.46	0.48

ARC-mode	Control	A	B	C
NO_3	0.36	0.81	1.36	2.40
NO_2	0.00	0.00	0.00	0.25

A: 5 s. B: 10 s. C: 20 s.

optimum condition for the growth of the lipid globule was determined by varying the voltage. The DBD-mode discharge was observed from 7 to 10 kV.

The experimental results show that the nitric acid concentration is lower in the DBD mode at low power. In the arc- discharge started between the wire electrode and the water surface, (> 10 kV).

The increase in temperature was negligible after 5 - 10 s of the plasma treatment. The measurement of the concentration was performed using a high-performance liquid chromatograph, HPLC Prominence-ILC-2030 Plus (Shimadzu Co. Japan) installed with a UV detector and a reverse mode column: X-bridge C-18.5 μm.

3.3 Choice of the plasma treatment method

Figure 5 (Table 5) compares the plasma treatment in the *Lipomyces* mixture and the post-mixture of the plasma-treated medium. The yeast was separated in the centrifugal separator and mixed into the plasma-treated medium immediately.

The incubation period lasted for 4 days. The lipid globules shrank and the cell count increased in the plasma-treated media. The volume increased while the cell count decreased in the plasma treatment of the suspension with yeast compared with the control. This result indicates that plasma treatment in the suspension with yeast is a better selection in terms of lipid globule volume increase.

3.4 Optimization of the media

The lipid shrinks, when incubated in the plasma-treated media. We compared the volume of the lipid globule in the plasma treatment on 5 mL of (a) peptone, (b)

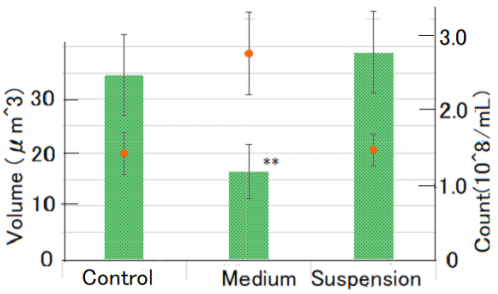

Fig. 5 Comparison of the volume of lipid globules and count between the plasma injection in suspension and post-injection medium, after cultivating for 6 days. Power source LHV-13AC; Stirrer: 120 rpm. $** p < 0.01$ (Dunnett's method).

Table 5 Comparison after the cultivation (6 days).

	Control	PTM	Yeast suspension
Volume (μm^3)	34.6	16.5	38.9
Count of cells (10^8 cells/mL)	1.39	2.70	1.44

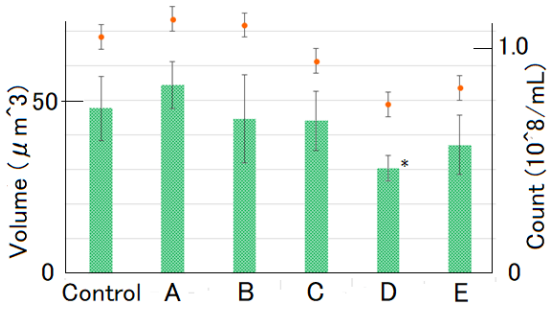

Fig. 6 Comparison of the volume of lipid globules and cell count in various media. Power source: LHV-10AC-24; Stirrer: 120 rpm. $*p < 0.05$ (Dunnett's method).

Table 6 Cultivation in various media.

	Control	A	B	C	D	E
Volume	47.7	54.4	44.7	44.0	30.3	37.1
Count	1.03	1.10	1.08	0.92	0.73	0.80

Medium A: peptone; B: yeast extract; C: glucose; D: malt extract; E: water. Volume in μm^3 and count in 10^8 cells/mL.

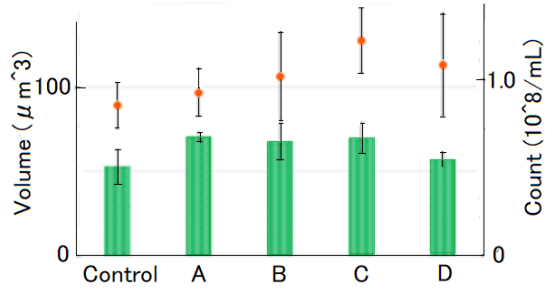

Fig. 7 Volume of lipid globule for various excitation voltage. Plasma injection on yeast mixture in 1/2 YM medium, 5 mL. Power source: LHV10AC-24; stirrer frequency: 120 rpm.

Table 7 Dependence on the excitation voltage.

	Control	A	B	C	D
Volume	53.1	70.6	67.9	69.9	57.2
Count	0.77	0.54	0.92	1.10	0.98

yeast extract, (c) glucose, (d) malt extract, and (e) water in the following experiment. These media were mixed with 1/2 YM media and *Lipomyces* and incubated for 5 days. Figure 6 (Table 6) shows the volume of the lipid globule and the cell count in various media. Case A, peptone, a soluble protein formed in the protein digestion, yields the best result, whereas Case D, malt extract, yields the worst result. The main composition of the malt extract is maltose. The research line was selected from agricultural produce, such as single sugar, and the evaluation was performed along this line.

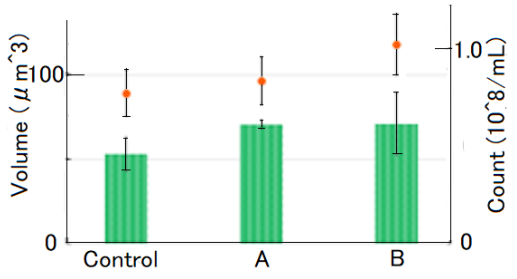

Fig. 8 Comparison of the lipid globule volume low dose conditions, at 7 kV, A: 5 s; B: 10 s. Power source: LHV-10AC-24; stirrer: 120 rpm.

Table 8 Comparison of plasma process.

	Control	A	B
Volume (μm^3)	53.1	70.6	67.9
Count (10^8 cells/mL)	0.77	0.84	1.02

Excitation voltage 7 kV, A: 5 s.; B: 10 s.

Figure 7 (Table 7) shows the volume of the lipid globule and the cell count at various excitation voltages. According to this viewpoint, the best result was Case A, at 7 kV, where the bar graph represents the largest volume of the lipid.

3.5 Optimization of the plasma treatment

Figure 8 (Table 8) shows the relationship between the volume of lipid globules and the number of cells in the 1/2 YM medium and the exposure time. The volume increases by 132% and the number of cells by 109%. The medium was selected from the standard mixture. In the search for a better result, a special mixture of YPD was found. Figures 9 and 10 show the experimental results.

Figure 9 (Table 9) shows the comparison of the plasma treatment of the separated medium without the yeast. In the plasma-treated media, yeast was separated from the medium by a centrifugal separator and mixed immediately after the plasma treatment.

Although the yeast did not suffer electrical interference damage, the incubation results showed that the size of the lipid globules increased to 1.13, and the number of cells decreased to 0.86 in terms of the control. The overall production efficiency was 0.98.

Figure 10 (Table 10) compares the plasma treatment in the suspension with yeast, where the volume of the lipid globules increased to 1.35 and the population of cells to 1.16. The overall production efficiency increased to 1.56.

The results show that a lower concentration of sugar is required to reduce the negative effect of plasma oxidation.

In the aeration of the liquid, part of the flue gas reacts with the liquid mixture, through the thin surface of bubbles. We focus on the primary reaction processes following Locke *et al.* [12], Mededovic and Locke [13] in the

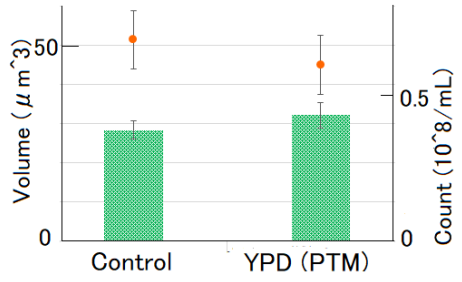

Fig. 9 Comparison of the volume of lipid globules and count, incubated in YPD (PTM), and lower concentration of sugar. Power source: LHV-10AC-24, Stirrer: 110 rpm. Incubation time: 5 days.

Table 9 Cultivation in YPD (PTM).

	Control	PTM
Volume (μm^3)	28.4	32.2
Count of cells (10^8 cells/mL)	0.69	0.60

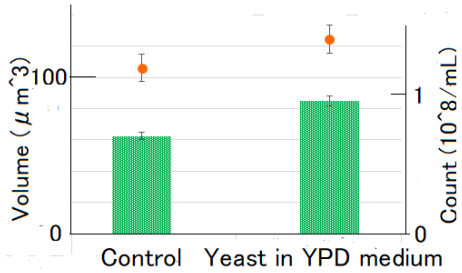

Fig. 10 Comparison of the volume of lipid globules and cell count. Plasma injection in yeast mixture in YPD mediem. Power source: LHV-10AC-24; stirrer: 110 rpm. Incubation time: 6 days.

Table 10 Cultivation, plasma-treat, yeast in YPD.

	Control	Yeast mixture
Volume (μm^3)	62.4	84.8
Count of cells (10^8 cells/mL)	1.2	1.4

discharge plasma in gas–liquid mixtures.

DBD generates NO and NO_2 in the gas phase from nitrogen, and when they react with oxidants, such as hydroxyl radicals in the liquid phase, nitrates and nitrites are generated, as in the following form:

Although the reaction of these nitrogen radicals is unknown, we assume that the following reactions occur in the DAS region:

Nitrogen reactions including the ozone quench generating the excited state of nitrogen and NO_x:

$$N_2 + e \rightarrow 2N^* + e,$$
$$O(^1D) + NO \rightarrow NO_2,$$
$$N^* + O_3 \rightarrow NO + O_2.$$

Reactions related to NO_2^- and nitrous acid, related to the production of nitrite ions and ONOO, and peroxy-nitrite play important roles.

$$NO_2^- + H_2O_2 \rightarrow ONO_2^-,$$
$$HNO_2 + H_2O_2 \rightarrow HOONO + H_2O.$$

The advanced oxidation by oxygen radicals is described in the following process. In the bubble region, electrons, atomic oxygen hydroxyl radicals, and nitrogen radicals are mixed with water vapor and the liquid.

Dissociation and ionization generating $^*OH$:

$$\begin{cases} H_2O + e \rightarrow OH^- + H^+ + e \\ H_2O + e \rightarrow {}^*OH + {}^*H + e \end{cases}.$$

High-over-voltage breakdown in the dry air region produces oxygen atoms, and hydroxyl radicals and ozone are produced in the chain reaction.

Reactions include excited oxygen

$$\begin{cases} O(^1D) + H_2O \rightarrow 2OH^* \\ O(^1D) + O_2 \rightarrow O_3 \end{cases}.$$

Reactions include metastable states of nitrogen molecules:

$$N_2(A^3\Sigma) + H_2O \rightarrow N_2 + {}^*OH + {}^*H.$$

Inhibition of O_3 production and enhancement of OH^* formation:

$$OH^- + O_3 \rightarrow {}^*O_2^- + HO_2^*,$$
$$O_3 + 3HO_2^* \rightarrow 3OH^* + 3O_2.$$

Production of superoxide: The oxygen molecule is the primary acceptor of electrons and forms $^*O_2^-$:

$$O_2 + e \rightarrow {}^*O_2^-.$$

Production of radicals:

$$\begin{cases} {}^*O_2^- + H_2O \rightarrow OH^- + {}^*HO_2 \\ {}^*HO_2 + {}^*HO_2 \rightarrow H_2O_2 + O_2 \\ H_2O_2 + {}^*O_2^- \rightarrow {}^*OH + OH^- + O_2 \\ H_2O_2 + e_{aq}^- \rightarrow {}^*OH + OH^- \end{cases}.$$

The aqueous electron–molecule reaction shows the reaction rate: $10^{10}\,M^{-1}s^{-1}$. $^*OH$ is produced in the dissociation of hydrogen–peroxide by the electron collision in the gas discharge.

Computer chemistry can expand the oxidation of natural sugar in the liquid region, for example, glucose.

Advanced oxidation produces gluconic acid:

$$\text{Glucose} + \{{}^*OH\} \rightarrow \text{Gluconic acid}.$$

Radical molecule reaction shows the reaction rate: 10^8 - $10^{10}\,M^{-1}s^{-1}$.

Glucose has three types: six-member ring, five-member ring, and linear. The acidity of the culture solution is caused by nitric acid and nitrite, which are produced during the gas oxidation reaction. Fat production

increases because of the reproduction of strong individuals who have overcome this stimulus. Gluconic acid also had a negative effect. Despite the importance of the liquid phase reaction, less is known about collision processes or high-energy radical reactions occurring in water. Figure 11 shows the electrophilic reaction susceptibility surface of glucose six-member ring alpha type. The electrophilic susceptibility of the dehydration reaction is this tendency. We calculated the electron affinity and LUMO/HOMO energy of organic molecules in water using Biomedical CAChe 6.0 to estimate the behavior of radical reactions in liquid media.

The effect in water was adjusted using the dielectric constant around the molecule. The possibility of this reaction depends on the HOMO energy of glucose −11.050 eV and the LUMO energy of 2.149 eV. The production of gluconic acid can be explained using quantum chemistry.

In the thermodynamic equilibrium, the energy difference between the LUMO energy and the singly occupied molecular orbit of OH^* is used to determine the direction of the reaction. The difference in the energy level between the glucose and OH^* is as follows:

$$LUMO\ 2.149\,eV < SUMO,\ OH^*\ 3.121\ eV.$$

Quantum-chemistry (CAChe calculations) revealed that the six-member ring α-glucose shows a −11.050 eV HOMO energy and a 2.149 eV LUMO energy. Gluconic acid shows a −10.873 eV HOMO energy and a 1.115 eV LUMO energy [14, 15]. If the reaction energy of radical is greater than the binding energy of –C–HOH– hydrogen constituting the annulus of glucose, dehydration by electron affinity reaction results in cleavage, and –O = C–OH.

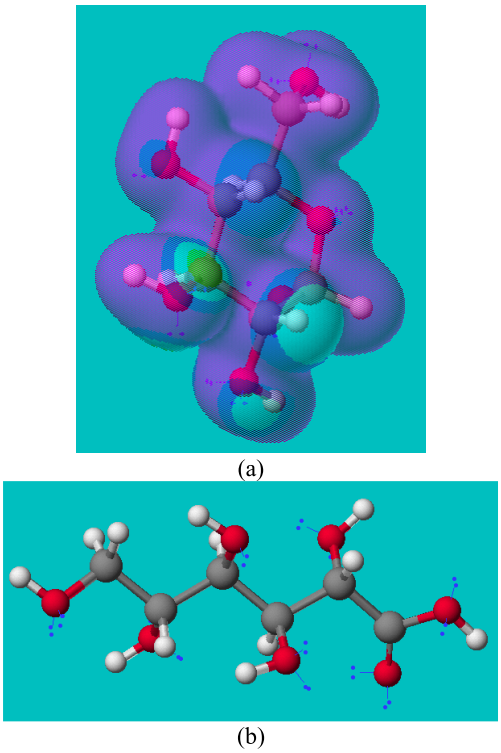

(a)

(b)

Fig. 11 Glucose and gluconic acid. (a) Molecular structure and the electrophilic susceptibility of six-member ring α-glucose. HOMO energy is −11.050 eV and LUMO energy is 2.149 eV. (b) Molecular structure of gluconic acid. HOMO energy is −10.873 eV, and LUMO energy is 1.115 eV [14, 15].

This change is related to the production of carboxylic acid-containing gluconic acid. The hydroxyl radicals play an important role in high-energy radical reactions, and oxidized glucose probably inhibits the growth of the yeast. However, it is also useful as a hydroxyl radical scavenger. The acidity and probably the electric field can influence the yeast and separate stronger individuals if the yeast can overcome this effect.

4. Conclusive Remark

This study evaluates the possibility of inducing lipid cell growth in the culture medium by irradiating it with liquid–gas boundary dielectric barrier plasma for several seconds and to determine the recovery media to be used for plasma treatment and excitation conditions. Rather than being limited to the culture solution, when exposed to a suspension containing yeast, lipid globule volume increased after many cells were recovered. In this study, a floating medium cultured with YPD and 1/2 YM medium was subjected to a saturation period in which the medium containing glucose content is reduced. The plasma treatment in the 1/2 YM medium increased the lipid globule volume.

According to the experimental findings, fewer sugar components are more effective, and sugar components such as glucose and maltose are denatured to oxidants under the influence of plasma treatment. The causes of the reduction in lipid globule volume due to plasma treatment of sugar components must be better understood, as well as the effects of oxidation of other components such as proteins. To achieve this, large-scale monolithic agriculture in the tropical rainforest can be replaced by Jar Fermenter culture. The study scheme prioritizes the rate of increase in lipid spherical volume as a proliferation promoter and then selects conditions that increase the number of cells. We hope that future research will enable lipid synthesis technology using the yeast *Lipomyces starkeyi* to overcome all issues and contribute to society.

Acknowledgments

The authors express special thanks to Ms. Dr. Mana Yanagiba and Dr. Takafumi Naganuma for their kind advice and for the alienation of the *Lipomyces starkeyi* CBS1807(T). Mr. Shiki Sato and Mr. Yawara Shiina are warmly acknowledged for their technical assistance. This work was supported in part by the Institute of Future Science, Akasaka, Tokyo, Japan.

[1] R.L. Starkey, "Lipid Production by a Soil Yeast", J. bacteriology, 33 (1946).
[2] T. Naganuma and Y. Uzuka, "Development of a new chemically defined sporulation medium for the yeasts in the genus Lipomyces", J. Gen. Appl. Microbiol. **43**, 5, 289 (1997), doi.org/10.2323/jgam.43.289.
[3] T. Naganuma, Y. Uzuka and K. Tanaka, "Quantitative Estimation of Intercellular Neutral Lipids of the Yeast, Lypomyces starkeyi", Agric. Biol. Chem. **46**, 1213 (1982), doi.org/ 10.1271/bbb1961.46.1213.
[4] Private communication, Takafumi Naganuma, "Challenge to Fat Mass – Production of YeastLipomyces", (2012).
[5] M. Yanagiba, T. Naganuma and K. Masaki, "Meaning and Research on Lipid Production for Biodiesel Fuel by Yeast Lipomyces and Trends in Microbial Lipid Production Research", Oleoscience **17** (3), 117 (2017), doi.org: 10.5650/oleoscience.17.117. (in Japanese)
[6] M. Yanagiba, K. Masaki, H. Shinmori and T. Naganuma, "Screening for Lipomyces strains with high ability to accumulate lipids from renewable resources", J. Gen. Appl. Microbiol. **65**, 80 (2018), doi.org/10.2323/jgam.2018.05. 006.
[7] M. Yanagiba, H. Shinmori and T. Naganuma, "Investigation of liquid culture conditions for triacylglycerol production from waste peach by Lipomyces wild-type strain", J. Oleo Sci. **68** (3) 245 (2019), doi.org/10.5650/jos.ess18168.
[8] T. Akitsu, S. Kojima, K. Katayama-Hirayama, S. Ogura, H. Okawa and K. Uno, "A Study on the Detection of Plasma Generated Radicals in the Degradation of Dibromophenols in Water Solution", The 28th International TOKI Conference on Plasma and Fusion Research, Toki, 11. 5-8, in 2019, Poster P1-44.
[9] H. Okawa, Y. Shiina, S. Kojima, K. Katayama-Hirayama and T. Akitsu, "Comparison of the Degradation Efficiency of Dinitrophenols in Dielectric Barrier Discharge at Gas/Liquid Boundary", Plasma Fusion Res. **16**, 1406070 (2021), doi.org/10.1585/pfr.16.1406070
[10] B. Sun, M. Sato and J. Clements, "Use of a pulsed high-voltage discharge for removal of organic compounds in aqueous solution", J. Phys. D: Appl. Phys. **32**, 15, 1908 (1999). Doi: 10.1088/0022-3727/32/15/319
[11] K. Oehmigen, M. Hähnel, R. Brandenburg, Ch. Wilke, K.D. Weltmann and Th. von Woedtke, "The Role of Acidification for Antimicrobial Activity of Atmospheric Pressure Plasma in Liquids", Plasma Processes Polym. **7**, Issue 3-4, 250 (2010), Doi.org/10.1002/ppap.200900077
[12] B.R. Locke, M. Sato, P. Sunka, M.R. Hoffmann and J.-S. Chang, "Electrohydraulic Discharge and Nonthermal Plasma for Water Treatment", Ind. Eng. Chem. Res. **45**, 882 (2006), doi.org/10.1021/ie050981u
[13] S. Mededovic and B.R. Locke, "Primary chemical reactions in pulsed electrical discharge channels in water", J. Phys. D. Appl. Phys. **40**, 7734 (2007), Doi.org/10.1088/ 0022-372740/24/021-
[14] Biomedical CAChe 6.0 User's Guide 2003, Fujitsu.
[15] K. Somekawa, "Molecular Orbital Calculation of Organic Molecules and the Application", Kyushu University Press, Fukuoka, Japan, 2013, ISBN 978-4-7985-0089-8.